Dynamical transition, hydrophobic interface, and the temperature dependence of electrostatic fluctuations in proteins

David N. LeBard and Dmitry V. Matyushov
Center for Biological Physics, Arizona State University, P.O. Box 871604, Tempe, Arizona 85287-1604, USA
(Received 28 July 2008; published 1 December 2008)

Molecular dynamics simulations have revealed a dramatic increase, with increasing temperature, of the amplitude of electrostatic fluctuations caused by water at the active site of metalloprotein plastocyanin. The increased breadth of electrostatic fluctuations, expressed in terms of the reorganization energy of changing the redox state of the protein, is related to the formation of the hydrophobic protein-water interface, allowing large-amplitude collective fluctuations of the water density in the protein's first solvation shell. On top of the monotonic increase of the reorganization energy with increasing temperature, we have observed a spike at $\simeq$220 K also accompanied by a significant slowing of the exponential collective Stokes shift dynamics. In contrast to the local density fluctuations of the hydration-shell waters, these spikes might be related to the global property of the water solvent crossing the Widom line or undergoing a weak first-order transition.

DOI: 10.1103/PhysRevE.78.061901 PACS number(s): 87.14.E−, 87.15.N−, 87.15.Pc

I. INTRODUCTION

A dynamical transition has been observed in many hydrated biopolymers, including proteins, DNA, and RNA [1–4]. It amounts to a sharp change in the temperature slope of the mean-squared atomic displacements of the biopolymer atoms at a temperature usually observed in the range $T_{tr}=200-230$ K. While the microscopic origin of this dynamical transition is still debated [5–9], an important open question is whether the existence of this universal property of hydrated biopolymers [10] can be connected to their specific functions at physiological temperature [1,2,10,11].

Electrostatics is significant to the catalytic action of enzymes [12,13]. Therefore, a link between a protein's dynamical transition and enzymatic activity may be reflected by some property characterizing electrostatics at the active site. It is currently well established that the dynamical transition is not observed in dry proteins, and its existence is universally attributed to the interaction of water with the protein interface. A property sensitive to the dynamical transition needs to connect water's electrostatics to the protein's active site. Here, we consider one such parameter which critically affects the barriers of protein redox reactions, the reorganization energy of electron transfer [14].

The reorganization energy λ of electronic transitions between proteins characterizes the breadth of thermal fluctuations of the energy gap ΔE between the donor and acceptor energy levels,

$$\lambda = \beta\langle(\delta\Delta E)^2\rangle/2. \tag{1}$$

Here, $\delta\Delta E$ is the fluctuation of the energy gap ΔE and the inverse temperature $\beta=1/(k_B T)$ corrects for the proportionality of the variance to temperature following from the fluctuation-dissipation theorem [15]. The reorganization energy λ is then typically a weak function of temperature when measured for electronic transitions in small molecules dissolved in dense polar solvents [16].

Experimentally accessible reorganization energy of inter-protein electron transfer [17] characterizes the coupling of the energy levels of both the donor and acceptor to the thermal bath. For long-distance electron transfer, most common in biological energy chains, λ can be split into a sum of individual, donor and acceptor, components and a Coulomb correction. Since these individual components mostly characterize the physics of the problem, our focus here is on the electrostatic fluctuations at the active site of a single protein.

Electron transfer changes the redox state of the protein and thus the partial atomic charges q_j of the active site. The electrostatic interactions of active site charge differences Δq_j with the potential of hydrating water $\phi_{w,j}$ at atomic sites j contribute to the Coulomb shift ΔE_w^C, which is a part of the overall donor-acceptor energy gap:

$$\Delta E_w^C = \sum_j \Delta q_j \phi_{w,j}. \tag{2}$$

Here, the sum runs over the atoms of the active site. The variance of this Coulomb energy gap calculated for the charges Δq_j of the active site of a single protein is what is studied in this paper. The water reorganization energy is then defined as

$$\lambda_w = \beta\langle(\delta\Delta E_w^C)^2\rangle/2. \tag{3}$$

The dynamical dimension of the problem is characterized by the normalized Stokes shift correlation function [18]

$$S_w(t) = \langle \delta\Delta E_w^C(t)\,\delta\Delta E_w^C(0)\rangle/\langle[\delta\Delta E_w^C(0)]^2\rangle, \tag{4}$$

where angular brackets denote an ensemble average. The common form of $S_w(t)$ in dense polar liquids includes a fast one-particle component with a Gaussian decay followed by exponential (or stretched exponential) decay describing collective solvent dynamics [18],

$$S_w(t) = A_G e^{-(t/\tau_G)^2} + (1-A_G)e^{-(t/\tau_E)^{\beta_E}}. \tag{5}$$

Here, τ_G and τ_E are, respectively, the Gaussian and exponential relaxation times and A_G quantifies the relative weight of single-particle dynamics in the reorganization energy; β_E is the stretching exponent.

The main result of the molecular dynamics (MD) simulations presented here is to show that the reorganization energy

$\lambda_w(T)$ rises significantly with temperature to a value much exceeding both the common estimates of this parameter for reactions involving small redox molecules [14] and previous estimates for protein electron transfer [12]. We associate this increase with formation of a hydrophobic interface allowing large-amplitude fluctuations of the local water density. We also show that both the long-time exponential relaxation time [τ_E in Eq. (5)] and the water reorganization energy λ_w pass through peaks at the temperature of dynamical transition T_{tr}=220 K. This special temperature (at atmospheric pressure) has been previously associated with a thermodynamic singularity in the phase diagram of bulk water [19,20]. It has also been associated with a crossover from fragile to strong dynamics of hydrated biopolymers [5,21,22].

II. MD SIMULATIONS

MD simulations reported here have been done for the redox metalloprotein plastocyanin (PC) from spinach according to the simulation protocol described in our previous publication [23]. PC is a single polypeptide chain of 99 residues forming a β sandwich, with a single copper ion ligated by cysteine, methionine, and two histidines. The protein's active site in our analysis is composed of a copper ion and four atoms (two nitrogens and two sulfurs) coordinating it. The partial charges on these atoms in both reduced (Red) and oxidized (Ox) states can be found in Ref. [24].

The initial configuration of PC was taken from a protonated x-ray crystal structure with a 1.7 Å resolution (Protein Data Base 1ag6 [25]). First, the initial protein configuration was minimized in vacuum using the conjugate gradient method for 10^4 steps to remove any bad contacts. Then, the system was solvated in an octahedral box with N_w=5886 TIP3P (transferable intermolecular potential, three-position model) molecules [26], providing at least two solvation shells around the protein. The protein was simulated in the Ox state with a total charge of −8 and in the Red state with the total charge of −9. In both cases, eight or nine sodium ions were added to neutralize the system, as is required for the Ewald summation. After adding the water and counterions, the system's energy was minimized for another 10^4 steps while the protein was allowed to relax and the water and sodium atoms were positionally constrained. Finally, the entire system was additionally minimized for 10^5 steps.

Following minimization, the system was heated in an *NVT* ensemble for 30 ps from 0 K to the desired temperature. Temperature equilibration was followed by a 2 ns density equilibration in an *NPT* ensemble at P=1 atm. This equilibrated structure was then used for 22 individual simulations of the Ox state and seven simulations of the Red state of PC to create 10 ns long trajectories. Temperature T was varied from 100 to 300 K at constant volume V and constant number of water molecules N_w. The total simulation time was 348 ns and required 7.4 CPU years, while only 270 ns were used for the production data analysis which lasted another 2.4 CPU years. The time step for all MD simulations was 2 fs, and SHAKE was used to constrain bonds to hydrogen atoms. Constant temperature and pressure simulations employed the Berendsen thermostat and barostat, respectively [27]. The long-range electrostatics were calculated using a smooth particle mesh Ewald summation with a 9 Å limit in the direct space sum.

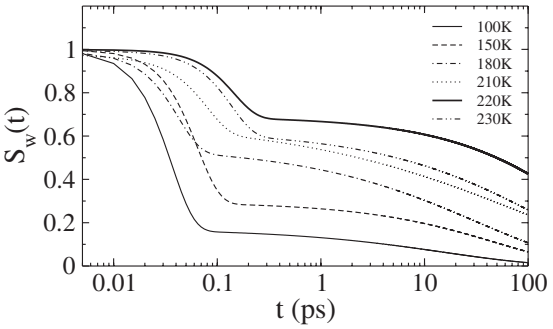

FIG. 1. Stokes shift correlation function of PC (Ox) at different temperatures indicated in the plot.

III. RESULTS

Most MD results reported here have been obtained from configurations in equilibrium with the Ox state of PC; the Stokes shift data were collected from both Ox and Red equilibrium trajectories as discussed below. We employed two observation windows to calculate the reorganization energies $\lambda_w(T)$ of PC(Ox) state, 1 and 10 ns. The latter length corresponds to the entire MD trajectory, while the former needs more explanation. When employing the 1 ns window, the reorganization energy is calculated from the variance of the Coulomb energy gap [Eq. (3)] by sliding a 1 ns observation window along a longer MD trajectory and averaging over the results of the variance calculations on each window. The average $\langle \Delta E_w^C \rangle_{obs}$ required to calculate the variance is not a global average but is obtained separately from each observation window. This approach to the calculation of averages is analogous to a laboratory procedure with a fixed resolution and is required for studies of systems with broad distributions of relaxation times [23]. In case of proteins, a subset of nuclear motions is always frozen on the simulation time scale and so both specifying the observation window and keeping it constant for all measurements is significant in maintaining consistent conditions for collecting the data.

Fits of the simulated Stokes shift functions to Eq. (5) are shown in Fig. 1. Two features are most prominent there: the increase of the relative importance of the collective solvent dynamics with increasing temperature [decrease of A_G in Eq. (5)], and the appearance of a peak in the exponential relaxation time at T_{tr}=220 K [Fig. 2(b)]. The exponential part of the reorganization energy $\lambda_E=(1-A_G)\lambda_w$ also shows a peak at the same temperature [inset in Fig. 2(a)].

Overall $\lambda_w(T)$ strongly increases from a value typical for short MD simulations of proteins [12] to a much larger value at higher temperatures [Fig. 2(a) and Table I]. The temperature of the onset of the $\lambda_w(T)$ rise is much below T_{tr}, at about 150 K commonly associated with the onset of rotation of methyl groups of protein's side chains [8,28]. This onset temperature however depends on the observation window. Since the relaxation times of the protein are widely different,

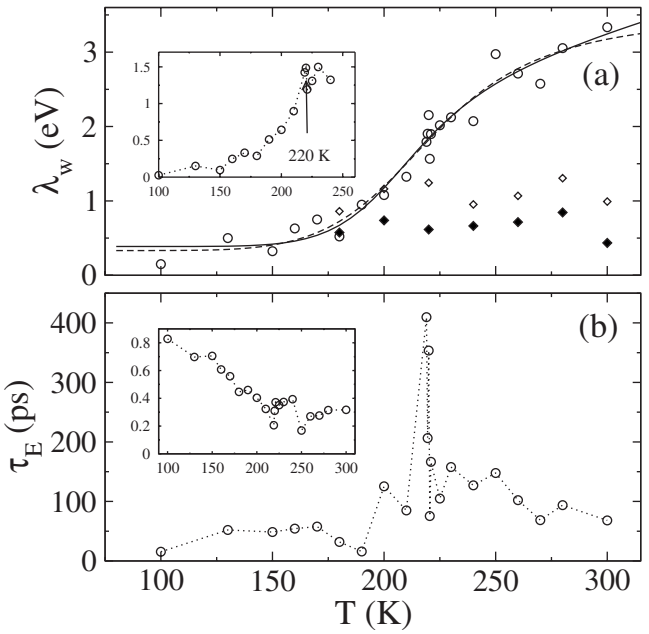

FIG. 2. (a) Circles indicate the water reorganization energy λ_w from MD simulations of PC (Ox) and the solid line shows the fit of the simulation data to Eq. (7) with the fitting parameters: $\lambda_G=0.39$ eV, $\lambda_{eq}=0.87+0.0084T$ eV, $\tau_{obs}/\tau_0=7350$, and $E_a=1867$ K; the dashed line assumes temperature-independent λ_{eq}. The inset shows the exponential part of the reorganization energy $\lambda_E=(1-A_G)\lambda_w$ produced by collective water fluctuations. The closed diamonds refer to half of the Stokes shift [Eq. (8)] and the open diamonds show the linear-response reorganization energy λ_w^{Ox} obtained from Eq. (9). (b) Exponential relaxation time of the Stokes shift correlation function obtained from MD of PC(Ox) and the Gaussian amplitude A_G in Eq. (5) (inset). The dashed lines connect the points.

the rise of $\lambda_w(T)$ is caused by the appearance of a particular relaxation mode in the observation window, methyl rotations in this case. However, we believe that the underlying picture is more complex and the main rise of $\lambda_w(T)$ is caused not by methyl rotations, but by a more collective mode coupled to the solvent interfacial translations [29,30] (see below). In fact, recent extensive simulations of the mean-squared atomic displacements of myoglobin [28] have reveled two breaks in the temperature slope: the first break at 150 K related to methyl (anharmonic) rotations followed by a stronger solvent-induced break at 220 K.

The appearance of a relaxation mode in the observation window restores the statistical ergodicity for that particular mode. The nonergodic rise of $\lambda_w(T)$ to its equilibrium value $\lambda_{eq}(T)$, also seen for model charge-transfer chromophores [31], can be described by imposing a stepwise frequency filter on the spectrum of Stokes shift fluctuations [16],

$$\lambda_w(T) = 2\lambda_{eq}(T)\int_{1/\tau_{obs}}^{\infty} S_w(\omega)d\omega. \quad (6)$$

Here, τ_{obs} is the observation window and $S_w(\omega)$ is the Fourier transform of the Stokes shift correlation function in Eqs. (4) and (5). In order to provide a physically transparent form for

TABLE I. Properties of hydrated plastocyanin (Ox) and TIP3P water in the simulation cell from MD simulations.

T (K)	λ_w [a]	λ_w [b]	$\langle N_I\rangle$	$\langle(\delta N_I)^2\rangle$	p_2	D [c]	τ_E [d]
100	0.15	0.57	568	20	−0.015	0.032	15.5
130	0.50	0.61	556	24	−0.022	0.003	52.0
150	0.32	0.75	561	32	−0.025	0.017	48.6
160	0.63	0.66	553	30	−0.021	0.015	54.3
170	0.75	0.93	555	42	−0.030	0.038	57.8
180	0.52	1.13	554	52	−0.025	0.041	32.0
190	0.95	1.03	552	61	−0.025	0.020	15.9
200	1.08	1.66	549	61	−0.027	0.037	125.5
210	1.33	2.40	541	60	−0.027	0.061	84.9
219	1.79	3.44	544	66	−0.025	0.088	409.6
219.5	1.90	7.74	538	75		0.053	206.4
220	2.15	6.66	537	71	−0.021	0.093	353.6
220.5	1.57	4.67	538	76		0.055	75.6
221	1.90	5.62	545	70	−0.025	0.095	166.5
225	2.02	4.49	537	78	−0.021	0.107	104.8
230	2.12	4.21	545	72	−0.021	0.126	157.8
240	2.07	5.27	539	80	−0.020	0.165	127.0
250	2.97	6.33	535	86	−0.020	0.206	147.8
260	2.71	3.98	530	88	−0.018	0.281	102.1
270	2.57	4.34	520	91	−0.016	0.326	68.5
280	3.05	3.83	507	96	−0.012	0.389	93.8
300	3.33	4.56	507	100	−0.014	0.536	68.1

[a]Water reorganization energies (in eV), obtained with $\tau_{obs}=1$ ns observation window.
[b]Water reorganization energies (in eV), obtained with $\tau_{obs}=10$ ns observation window.
[c]Diffusion coefficients of TIP3P water averaged over all molecules in the simulation box (in $Å^2/ps$).
[d]Exponential relaxation time (in ps) of the Stokes shift correlation function in Eq. (5).

$\lambda_w(T)$ one can consider an effective single-exponential Debye relaxation, instead of several relaxation modes, to characterize collective nuclear motions coupled to the Stokes shift dynamics. This procedure leads to the following simple relation:

$$\lambda_w(T) = \lambda_G + [\lambda_{eq}(T) - \lambda_G](2/\pi)\arctan[\tau_{obs}/\tau(T)], \quad (7)$$

where the effective Debye relaxation time is given by the Arrhenius law, $\tau(T)=\tau_0\exp(\beta E_a)$.

The Gaussian component of the solvent reorganization energy, related to ballistic water motions [18], is normally reasonably temperature independent [31]. On the other hand, the temperature decrease of $A_G(T)\simeq\lambda_G/\lambda_{eq}(T)$ in the fit of the Stokes shift function [inset in Fig. 2(b)] clearly points to the equilibrium reorganization energy increasing with temperature. From the anticipated relation of $\lambda_{eq}(T)$ with the variance of the number of particles in the first solvation shell, which linearly grows with temperature (see below), we have attempted a linear temperature dependence of $\lambda_{eq}(T)$ to fit the MD data to Eq. (7). The result is shown by the solid line in

Fig. 2(a), and it is not much different from the fit using a temperature-independent λ_{eq} [dashed line in Fig. 2(a)]. We also note that, since our simulation length obviously cuts some slow nuclear modes off, we have not used $A_G(T)$ from the fits of the Stokes shift correlation functions to calculate $\lambda_{eq}(T)$.

The activation energy E_a of an effective Debye mode obtained from the fit, E_a=1867 K, points to a secondary β-relaxation mode creating fluctuations of the electrostatic potential, in contrast to the primary α relaxation of the water-protein system with a commonly much higher activation barrier [32,33]. This activation energy is also lower than β relaxation of aqueous mixtures with the activation energy of the order of 5.5×10^3 K [9].

Also shown in Fig. 2(a) (closed diamonds) is the reorganization energy from the Stokes shift obtained from the difference of average Coulomb energy gaps in Ox and Red states:

$$\lambda_w^{\mathrm{St}} = \frac{1}{2}|\langle \Delta E_w^C \rangle_{\mathrm{Ox}} - \langle \Delta E_w^C \rangle_{\mathrm{Red}}|. \tag{8}$$

For water fluctuations following linear response one expects the reorganization energy from the variance [Eq. (3)] to be connected to the reorganization energy from the two first moments [Eq. (8)] by the following relation:

$$\lambda_w^{\mathrm{Ox}} = \lambda_w^{\mathrm{St}} - (\beta/2)\langle \delta\Delta E_w^C \delta\Delta E_P^C \rangle_{\mathrm{Ox}}. \tag{9}$$

In Eq. (9) we have stressed that the averages are taken over the configurations in equilibrium with PC(Ox) and ΔE_P^C is the Coulomb interaction energy of the difference charges of the active site [Δq_j, Eq. (2)] with the remaining partial charges of the protein matrix.

When a rigid molecule is solvated and the intramolecular energy gap (ΔE_P^C here) does not fluctuate, the second correlator in Eq. (9) is zero. One then arrives at the standard expectation of the linear solvation theories that two routes to the reorganization energy, from the second cumulant [Eq. (3)] and from two first cumulants [Eq. (8)], are equivalent [14,16]:

$$\lambda_w^{\mathrm{St}} = \lambda_w. \tag{10}$$

Since the protein matrix fluctuates itself, the cross correlation in principle needs be taken into account, and it turns out to be negative [34]. However, when the cross-correlation term is subtracted from λ_w^{St} in Eq. (9) [open diamonds in Fig. 2(a)], the result is still significantly below the reorganization energy from the variance [Eq. (3)]. We therefore observe here a severe breakdown of linear solvation.

What Fig. 2(a) in fact indicates is that the two definitions of the reorganization energy converge at low temperatures, while the reorganization energy from the variance deviates significantly upward from half the Stokes shift above $T\simeq200$ K. This observation implies that the fast water modes responsible for electrostatic fluctuations, presumably librations, which are still unfrozen at low temperatures, follow the expectations of the linear response theories. On the contrary, a slower collective mode, which appears in the observation window at higher temperatures and gives rise to the gigantic reorganization energy, does not follow the linear response. The cross correlation does not restore linear solvation, in contrast to an earlier observation made for a water-exposed tryptophan residue [34]. The low value of the cross correlation physically implies that elasticities of the protein and water are drastically different and their electrostatic fluctuations are mostly decoupled. From that perspective, this correlation decoupling should hold for any solute-solvent combination with significantly different rigidities.

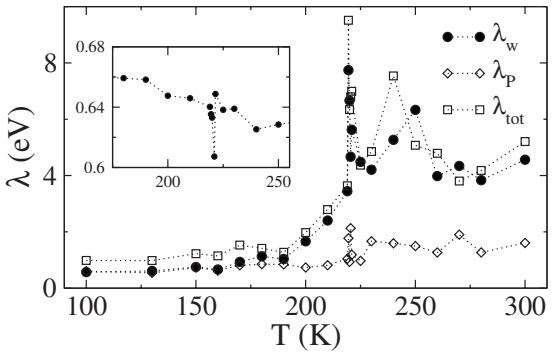

FIG. 3. Reorganization energy obtained from the variance of the Coulomb energy gap: water component λ_w [circles, Eq. (3)], the protein component λ_P from the variance of ΔE_P^C (diamonds), and the total water-protein reorganization energy λ_{tot} from the variance of the total Coulomb energy gap $\Delta E_w^C+\Delta E_P^C$ (squares). The inset shows the Binder parameter [35] built on the Coulomb interaction of the active site with hydrating water [Eq. (13)].

A spike of $\lambda_w(T)$ at $\simeq$220 K, barely seen on the 1 ns observation window, becomes more pronounced on the 10 ns time scale, as is shown in Fig. 3 where the reorganization energies for water, protein, and the full reorganization energy from the water-protein electrostatic fluctuations were collected from the entire 10 ns trajectories. The total reorganization energy is calculated from the variance of the total Coulomb energy gap $\Delta E_w^C+\Delta E_P^C$:

$$\lambda_{\mathrm{tot}} = \beta\langle(\delta\Delta E_w^C + \delta\Delta E_P^C)^2\rangle/2. \tag{11}$$

Since two energy gaps are involved in the variance, λ_{tot} (squares in Fig. 3) is a sum of individual water (λ_w, circles in Fig. 3) and protein (λ_P, diamonds in Fig. 3) components and, in addition, of a cross term λ_{Pw}:

$$\lambda_{\mathrm{tot}} = \lambda_w + \lambda_P + \lambda_{Pw}. \tag{12}$$

The increased amplitude of the peak seen from 10 ns trajectories suggests that it is produced by some slow, collective motions of water, significantly cut off on the 1 ns time scale and becoming more pronounced on a longer observation scale.

The question of the origin of the reorganization energy spike at about 220 K (which shoots up to an astonishing value of 10 eV) cannot be fully resolved based on our present simulations. It was previously suggested that an analogous, although much broader, maximum observed for the heat capacity of the hydrated protein might be related to crossing the Widom line of the bulk water [6]. An alternative explanation might involve a weak first-order transition in water [20]. Our data in fact lean more toward that second

explanation since we have observed a downward spike in the Binder parameter [35] built on the statistics of the energy gap fluctuations:

$$\delta_B = 1 - \langle (\Delta E_w^C)^4 \rangle / [3\langle (\Delta E_w^C)^2 \rangle^2]. \quad (13)$$

Crossing the Widom line, which sets the state of strongest cooperativity of bulk water, would suggest a thermodynamic singularity of the second-order type when the fluctuations at the transition point are still Gaussian. On the contrary, the parameter δ_B shows a downward spike from the value of 2/3 characteristic of Gaussian fluctuations (inset in Fig. 3). Such narrow downward spikes are often observed for first-order transitions, while its small depth testifies to the transition weakness (close to the critical point). In addition, no significant changes in the first moments of the energy gap ΔE_w^C were observed at the transition temperature (Stokes shift in Fig. 2), thus ruling out a strong first-order transition. We also note that δ_B shows a slow downward turn at temperatures above T_{tr}, in a general agreement with anticipated anharmonic, non-Gaussian character of the interfacial fluctuations at higher temperatures. Finally, Fig. 3 shows a spike in the protein reorganization energy λ_P at T_{tr}. Since this spike is much weaker than the corresponding spike of the water component, we believe that it does not reflect a property of the protein polymer itself, but can more likely be attributed to slaving of the protein fluctuations by hydrating water [33].

The fluctuations of water's electrostatic potential at the active site can generally be traced back to two weakly correlated nuclear modes in polar liquids, the orientational polarization, and the local density [36]. In order to clarify the origin of the dramatic rise of the reorganization energy, we have looked at two additional correlation functions characterizing the density and orientational manifolds of the water molecules in the protein's first solvation shell. A water molecule is defined as to belong to the first solvation shell if its oxygen atom is within 2.87 Å distance from the protein van der Waals surface.

The density manifold is characterized by the fluctuation of the number of particles $N_I(t)$ in the first solvation shell,

$$C_N(t) = \langle \delta N_I(t)\, \delta N_I(0) \rangle. \quad (14)$$

Further, the orientational manifold is described by the fluctuations of the total dipole moment $\mathbf{M}(t)$ of the water dipoles in the first solvation shell,

$$C_M(t) = \langle N_I \rangle^{-1} \langle \delta \mathbf{M}(t) \cdot \delta \mathbf{M}(0) \rangle, \quad (15)$$

where $N_I(T) = \langle N_I \rangle$ is the average number of first-shell waters. In $C_N(t)$ and $C_M(t)$, the fluctuations $\delta N_I(t)$ and $\delta \mathbf{M}(t)$ denote the deviations from the corresponding average values. The variances were calculated on the 1 ns observation window by using the same procedure as for the reorganization energy calculations presented in Fig. 2.

The temperature dependences of the average and variance of the number of waters in the first solvation shell (Fig. 4) are indicative of the formation of the hydrophobic protein-water interface with increasing temperature. The average $N_I(T)$ is generally a decaying function [Fig. 4(a)], and the slope of this decay becomes sharper above the transition temperature T_{tr} (see below). The decrease in the density of water at the interface allows stronger density fluctuations [Fig. 4(b)] and it is this regime of large interfacial density fluctuations that is a signature of hydrophobic solvation [37]. In this regime, one-particle exchanges of water molecules between the surface and the bulk [30] combine into large-scale collective density waves producing significant modulations of the electrostatic potential reflected in $\lambda_w(T)$. This thermal noise of hydrophobic surfaces is also reflected in a well-documented increase of protein's heat capacity upon unfolding, indicative of an increased breadth of the energy fluctuations [38,39].

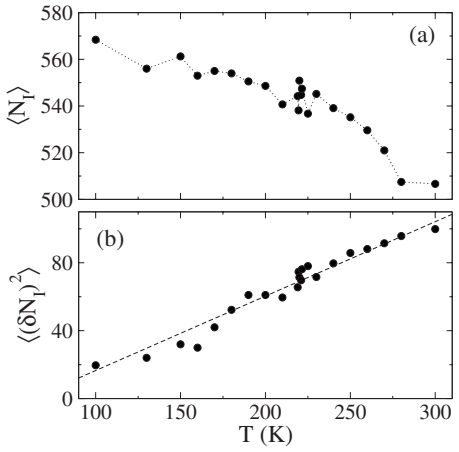

FIG. 4. Average number of water molecules in PC's first solvation shell (a) and its variance (b) vs temperature. The dashed line in (b) shows a linear regression through the points and the dotted line in (a) connects the simulation points.

The interfacial density fluctuations originate from the exchange of waters between the hydration shell and the bulk. These fluctuations can be represented as binding-unbinding events at the protein surface [40] with the resulting equilibrium reorganization energy $\lambda_{eq}(T)$ scaling linearly with the variance of the number of particles in the hydration shell: $\lambda_w(T) = a + b\langle (\delta N_I)^2(T) \rangle$, where coefficients a and b are weak functions of temperature. This expectation, used in the solid-line fit in Fig. 2(a), is corroborated quite well given the linear scaling of $\langle (\delta N_I)^2(T) \rangle$ with temperature [Fig. 4(b)]. A fairly significant temperature rise of $\lambda_{eq}(T)$ (see the fitting parameters in Fig. 2) also indicates a substantial density component in the overall reorganization energy at ambient conditions, in contrast to a 20–30 % contribution for small solutes in dense polar solvents [36]. We therefore conclude that the contribution to $\lambda_{eq}(T)$ from density fluctuations is significantly magnified by the soft and flexible nature of the hydrophobic protein-water interface.

The orientational fluctuations of the first-shell dipoles do not show a resolvable correlation with the reorganization energy (Fig. 5), but allow a deeper insight into the physics behind the electrostatic fluctuations inside the protein. The variance of the first-shell dipole moment grows with rising temperature, in accord with a general expectation of increased softness of the solvation shell, but does not show an obvious correlation with $\lambda_w(T)$. There is a weak maximum at T_{tr} for $\langle (\delta \mathbf{M})^2 \rangle$, but it is hard to assess from our data whether this is another reflection of the same spike seen for λ_w in Figs. 2(a) and 3.

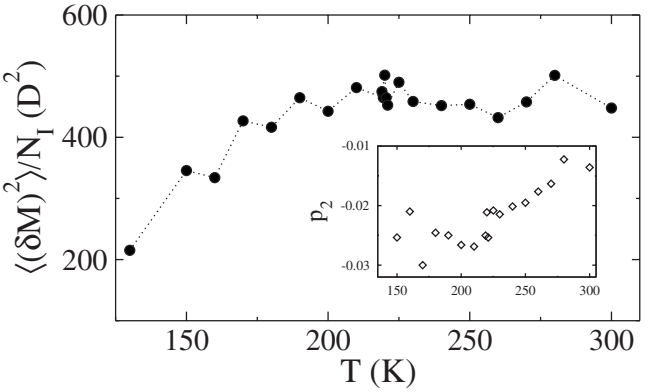

FIG. 5. $\langle(\delta M)^2\rangle/N_I(T)$ vs temperature. The inset shows the second-rank orientational order parameter $p_2(T)$ [Eq. (18)]. The dotted line connects the points.

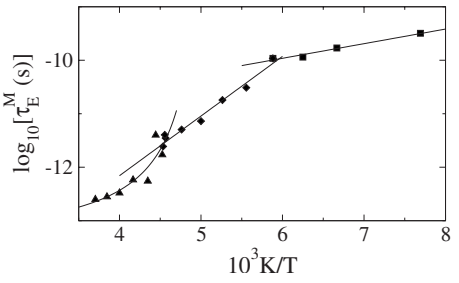

FIG. 6. Exponential relaxation time τ_E^M extracted by fitting the correlation function $C_M(t)$ from Eq. (15) to Eq. (5). The points are the simulation results in three ranges of temperature where they are fitted to the Vogel-Fulcher temperature law (at highest temperatures) and to Arrhenius laws (at the intermediate and lowest temperature ranges). The solid lines show the results of the fits.

A large magnitude of $\langle(\delta\mathbf{M})^2\rangle$ shown in Fig. 5 deserves a special comment. This correlation function can be re-written as follows

$$\langle N_I\rangle^{-1}\langle(\delta\mathbf{M})^2\rangle \simeq g_K\mu^2 - \langle N_I\rangle\langle\mu\rangle^2, \tag{16}$$

where $\langle\mu\rangle$ is the average dipole of the first-shell waters and μ=2.35 D is the magnitude of the dipole moment of TIP3P water. Further, we have introduced an analog of the Kirkwood factor of bulk dipolar liquids [41]

$$g_K = \sum_{k=1}^{N_I}\langle\hat{\mathbf{e}}_1\cdot\hat{\mathbf{e}}_k\rangle. \tag{17}$$

Here, $\hat{\mathbf{e}}_k$ is the unit vector of the first-shell water dipole and the approximate equality in Eq. (16) indicates that we have neglected the fluctuations of the number of first-shell waters for this discussion.

The MD simulations show a quite significant average dipole moment weakly decreasing with rising temperature and reaching the value of $\langle\mu\rangle$=0.36 D at 300 K. This average dipole moment is created by the asymmetric charge distribution of the protein polarizing its first solvation shell. PC's dipole moment is 2200 D (Ox) and 2470 D (Red) when calculated relative to the center of atomic partial charges. The induced permanent dipoles in the first solvation shell are highly correlated, which is reflected by the Kirkwood factor in Eq. (17) reaching the magnitude of 147 at 300 K. When this value is used in the Kirkwood-Onsager equation [41], it results is an effective dielectric constant of the hydration shell of about 4000. This estimate should not be confused with the macroscopic dielectric constant of the protein-water mixture, which is the only well-defined dielectric parameter, or with the commonly low effective dielectric constants assigned to the protein matrix [13]. We note, however, that very large values of the dielectric constant ($\simeq 10^4$ in Ref. [42]) originating from hydrating water monolayers are not uncommon in dielectric measurements of hydrated protein powders [42–45].

What this strong correlation between the first-shell dipoles physically means is that electrostatically the first solvation shell behaves as a flexible ferroelectric cluster, highly polarized by the protein electric field. Fluctuations of the electrostatic potential within this cluster are then reflected by the water reorganization energy reported here. The dielectric response of this polarized shell is very different from the response of an unperturbed polar liquid to a probe dipole or charge studied by linear solvation theories and that is the fundamental reason for breaking the relationship between the first and second moments [Eq. (10)] anticipated by linear response theories.

The inset in Fig. 5 shows the second-rank orientational order parameter

$$p_2 = \left\langle \sum_{j\in I} P_2(\hat{\mathbf{e}}_j\cdot\hat{\mathbf{r}}_j)\right\rangle. \tag{18}$$

Here, $\hat{\mathbf{r}}_j$ is the unit vector along the direction connecting oxygen of water molecule j in the first solvation shell with the closest atom of the protein surface; $P_2(x)$ is the second Legendre polynomial. The vector $\hat{\mathbf{r}}_j$ is thus close to the normal to the van der Waals surface of the protein. The low-temperature portion of $p_2(T)$ is practically constant showing a slight preferential orientation of the water molecules parallel to the interface as has been previously observed at interfaces of nonpolar substances and proteins with water [46,47]. This preferential ordering decays with increasing temperature resulting in essentially random, on average, orientations of water dipoles relative to the surface normal. Since the vector $\hat{\mathbf{r}}_j$ runs over the entire protein surface, this observation does not contradict to the existence of an average dipole moment of first-shell dipoles induced by protein's asymmetric charge distribution.

We believe that large fluctuations of the first-shell dipole moment are caused by density flexibility of the protein-water interface. This assessment is supported by the data for exponential relaxation times of $C_N(t)$ and $C_M(t)$ obtained by fitting these correlation functions to Eq. (5). When both exponential relaxation times are fitted to Arrhenius laws, they produce activation energies of 1389 and 2076 K, respectively, in a close range with the activation energy of 1867 K obtained from the fit of $\lambda_w(T)$ to Eq. (7). We note that this activation barrier is consistent with the activation enthalpies

of 1400–2400 K obtained by a variety of techniques for β fluctuations of hydrated proteins [33] which are considered to be slaved by β fluctuations of the hydration shell [33,48]. One also needs to keep in mind that an average Arrhenius slope actually hides a fairly complex behavior. Figure 6 shows the exponential relaxation time of $C_M(t)$ vs inverse temperature. The low-temperature portion of the data (triangles) is well approximated by a non-Arrhenius Vogel-Fulcher temperature law. This is followed by what can be characterized as a fragile-to-strong crossover followed by yet another break in the Arrhenius slope at $\simeq$160 K. This picture is consistent with two breaks in the slope seen in the simulations of mean-squared atomic displacements of myoglobin [28], where the lowest-temperature break was associated with the onset of methyl group rotations. The results for exponential relaxation times of $C_N(t)$ are more scattered and we could not reach an equally informative conclusion except for the average Arrhenius slope.

IV. DISCUSSION

Many alternative explanations have been sought for the observed dynamical transition in biopolymers [10]. Given that the transition is not observed for dry protein samples, the possible scenarios are limited to either the protein-water interface or to a bulk property of water. The recent observations, from neutron scattering measurements, of the fragile-to-strong crossover in the dynamics of partially hydrated protein powder samples [5] point to the second (bulk water) scenario. The crossover, also seen in the recent simulations [6,22], can be connected to the bulk water crossing the Widom line, i.e., the line of maximum cooperativity of the water fluctuations [19]. On the other hand, other recent experimental data on quasielastic neutron scattering, dielectric relaxation [8], and conductivity [7] of hydrated proteins have not revealed any special points in the corresponding relaxation times around the temperature of dynamical transition. These latter data report the temperature dependence of the primary α relaxation of the protein-water system and therefore these authors have concluded that the observed dynamical crossover [5] should be attributed to the appearance of a secondary relaxation in the observation window at $T > T_{\mathrm{tr}}$ [8,48].

In addition, recent observations of the dynamical transition in DNA and RNA [21,49] have clearly shown that this property is not unique to a peptide-based polymer. These findings again reemphasize the notion that either a bulk property of water or some generic property of the interface, not much sensitive to the details of the macromolecular structure, is responsible for the transition. Our data in fact suggest that both bulk and interfacial views need to be invoked to explain different facets of the problem, but the interface aspect has a dominant effect.

We have shown that the dramatic rise of the reorganization energy correlates with the depletion of the first solvation shell and the related increase in the strength of the first-shell density fluctuations. Figure 7 additionally supports this view.

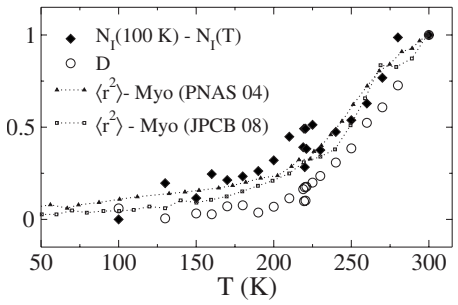

FIG. 7. Diffusion coefficient (open circles) from the present simulations and atomic mean-squared displacements of myoglobin measured experimentally [33] (small up triangles) and obtained from MD simulations [28] (small squares). Closed diamonds show the change in the number of particles in the first solvation shell (Fig. 3). All parameters are normalized to their corresponding values at 300 K.

Here we compare experimental [33] and simulated [28] atomic mean-squared displacements of myoglobin (small points) with our calculations of the diffusivity of water in the simulation box and the change in the number of waters in the first solvation shell. All parameters have been normalized to their corresponding values at 300 K to bring them to a common scale. The remarkable result of this comparison is that the average number of waters in the first solvation shell follows very closely the atomic displacements changing its temperature slope at the point of dynamical transition, T_{tr}=220 K. The increased mobility of the protein is therefore related to the increased translational mobility of waters [30,50] caused in turn by the creation of the high-temperature hydrophobic interface [37].

The diffusion coefficient of water in the simulation box is plotted separately vs the inverse temperature in Fig. 8, where we also compare our results to previous simulations by Kumar *et al.* [6] and by Lagi *et al.* [22]. The diffusion coefficient was calculated from the Einstein equation and the reported values are averaged over all waters in the simulation box. The different magnitudes of diffusivity compared to

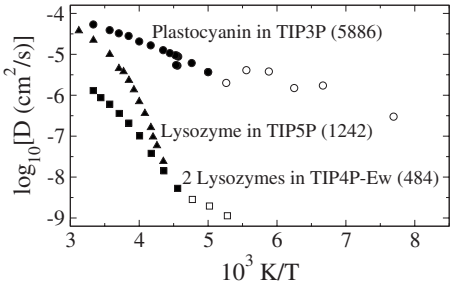

FIG. 8. Diffusion coefficient of TIP3P water calculated from all N_w=5886 water molecules in the simulation box (circles). The triangles indicate the results of Ref. [6] for the simulation box containing N_w=1242 waters; the squares denote the results from Ref. [22] with N_w=484 per simulation box containing two protein molecules. Closed and open points indicate temperatures above and below the dynamical transition temperature, respectively.

previous reports [6,22] are related to the different force fields used, but, more importantly, to the different fractions of water molecules in the simulation sample. Given that all molecules in the smallest sample in Fig. 8 belong to the interface [22], it is not that surprising that these data show the slowest diffusion, in agreement with the common expectation of slower diffusion of waters in thin interfacial layers [51]. Nevertheless, despite the use of a much larger number of waters (N_w=5886 vs N_w=484), we confirm here the existence of a crossover in the Arrhenius slope of water's diffusion coefficient observed earlier in Ref. [22].

Two observations are relevant in respect to the diffusivity data shown in Fig. 8. First, the temperature law is Arrhenius both above and below the transition temperature with the slope decreasing at lower temperatures, in accord with previous observations [5,22]. Second, the transition temperature is shifted down to 200 K compared to 220 K found in simulations of partially hydrated proteins in Ref. [22]. The first observation implies that we observe only a change in the character of a secondary, Arrhenius relaxation, as indeed often seen for electron transfer in proteins [11], instead of a fragile-to-strong transition. This fact might be related to the often reported [52] disappearance of α relaxation in confined water most closely related to our simulation conditions. Since $D(T)$ follows closely the decrease in the number of hydration-shell waters (Fig. 7) a connection of the break in the slope to a secondary process produced by collective density fluctuations of the hydration shell seems a reasonable explanation. The second feature might imply that the existence and position of the transition temperature depend on the fraction of surface waters in the system. While all waters in the simulation setup in Ref. [22] belonged to the surface, only roughly 10% of waters in our simulations find themselves in the first solvation shell (Fig. 4 and Table I). Likewise, we have obtained a fragile-to-strong crossover by considering only first-shell fluctuations in Fig. 6, but it is already washed out for the diffusivity averaged over several hydration layers.

Our data, while pointing mostly to the interfacial effects as the reason for the dramatic rise of $\lambda_w(T)$ and the dynamical crossover, do not entirely exclude a bulk thermodynamic singularity of water from the picture. While the global rise of the intensity of electrostatic fluctuations within protein is linked to the density fluctuations of the interface, the spike of $\lambda_w(T)$ at T=220 K and the corresponding slowing down of the Stokes shift relaxation might well be linked to the crossing of the Widom line or to a weak first-order thermodynamic transition. The first-order character can be a property of water [20,53] or be imposed by the protein. The latter possibility is consistent with the suggestion by Tournier and Smith [54] that just a few protein modes gain a multiminimum character above the transition. If the corresponding free energy curves for these modes have small biases between the minima, this picture would result in a first-order-type behavior if these modes are coupled to the interfacial water fluctuations. This latter scenario is supported by the increased harmonic character of these modes with increasing hydrostatic pressure [55], accompanied by the formation of water networks on the protein surface [56].

V. CONCLUSIONS

In conclusion, we have found a dramatic increase in the breadth of water-induced electrostatic fluctuations inside the protein with increasing temperature. We link this increase to the creation of a hydrophobic interface at extended hydrophobic patches of the protein. What has escaped the attention of all studies of the dynamical transition in biopolymers is the onset of hydrophobic solvation occurring at the same temperature T_{tr} as the dynamical transition. It might be true that the creation of the hydrophobic interface with its large extent of density fluctuations and intense electrostatic noise is closely linked to the dynamical transition, although we do not currently have any additional data supporting this view. However, if this view is correct, there should be a critical polypeptide dimension below which the macroscopic hydrophobic interface does not form [37] and no dynamical transition exists. In fact, very recent measurements of the terahertz dielectric response [57] of hydrated polypeptides of different lengths have indicated the existence of exactly such a critical polymer length below which the dynamical transition disappears.

We found that the dynamics of electrostatic fluctuations are coupled to fast β relaxation of the hydration shell. The redox activity of proteins can therefore be classified as hydration-shell coupled, according to the classification suggested by Fenimore *et al.* [33]. Although this coupling carries similarities with aqueous mixtures of simple glass formers [9], proteins are not just large molecules [58]. The formation of the hydrophobic interface is related to a particular length scale of hydrophobic patches ($\simeq$1 nm [37]) which does not exist for small hydrated molecules. Not surprisingly, large-amplitude electrostatic fluctuations observed here are not usually seen inside small molecules [16], although this feature might extend to other patchy hydrophobic surfaces, such as lipid membranes and dendrimeric structures.

Two factors peculiar to hydrated proteins might contribute to the large breadth of electrostatic fluctuations observed here. First, an extended hydrophobic interface allows large-amplitude density fluctuations enhanced by anharmonic protein motions. Second, strong polarization of the hydration dipoles by the asymmetric charge distribution of the protein creates a significant total dipole moment of the hydration layer. The polarized interface thus behaves like an "elastic ferroelectric bag" surrounding the protein and inducing a high-amplitude electrostatic noise inside it.

It remains to be seen whether and how the gigantic reorganization energy found at high temperatures is related to the biological function of metalloproteins belonging to energetic electron-transfer chains. One can anticipate, from a general perspective, that a significant increase in the amplitude of electrostatic fluctuations can help in reducing barriers for chemical transformations by allowing better chances for favorable configurations from a broad fluctuation spectrum.

ACKNOWLEDGMENT

This research was supported by the the NSF (Grant No. CHE-0616646).

[1] B. F. Rasmussen, A. M. Stock, D. Ringe, and G. A. Petsko, Nature (London) **357**, 423 (1992).
[2] A. L. Lee and A. J. Wand, Nature (London) **411**, 501 (2001).
[3] F. G. Parak, Rep. Prog. Phys. **66**, 103 (2003).
[4] G. Caliskan, R. Briber, D. Thirumalai, V. Garcia-Sakai, S. Woodson, and A. Sokolov, J. Am. Chem. Soc. **128**, 32 (2006).
[5] S.-H. Chen, L. Liu, E. Fratini, P. Baglioni, and E. Mamontov, Proc. Natl. Acad. Sci. U.S.A. **103**, 9012 (2006).
[6] P. Kumar, Z. Yan, L. Xu, M. G. Mazza, S. V. Buldyrev, S.-H. Chen, S. Sastry, and H. E. Stanley, Phys. Rev. Lett. **97**, 177802 (2006).
[7] S. Pawlus, S. Khodadadi, and A. P. Sokolov, Phys. Rev. Lett. **100**, 108103 (2008).
[8] S. Khodadadi, S. Pawlus, J. H. Roh, V. G. Sakai, E. Mamontov, and A. P. Sokolov, J. Chem. Phys. **128**, 195106 (2008).
[9] K. L. Ngai, S. Capaccioli, and N. Shinyashiki, J. Phys. Chem. B **112**, 3826 (2008).
[10] D. Ringe and G. A. Petsko, Biophys. Chem. **105**, 667 (2003).
[11] F. Parak, E. N. Frolov, A. A. Kononenko, R. L. Mössbauer, V. I. Goldanskii, and A. B. Rubin, FEBS Lett. **117**, 368 (1980).
[12] A. Warshel and W. W. Parson, Q. Rev. Biophys. **34**, 563 (2001).
[13] T. Simonson, Rep. Prog. Phys. **66**, 737 (2003).
[14] R. A. Marcus and N. Sutin, Biochim. Biophys. Acta **811**, 265 (1985).
[15] L. D. Landau and E. M. Lifshits, *Statistical Physics* (Pergamon, New York, 1980).
[16] D. V. Matyushov, Acc. Chem. Res. **40**, 294 (2007).
[17] H. B. Gray and J. R. Winkler, Proc. Natl. Acad. Sci. U.S.A. **102**, 3534 (2005).
[18] R. Jimenez, G. R. Fleming, P. V. Kumar, and M. Maroncelli, Nature (London) **369**, 471 (1994).
[19] L. Xu, P. Kumar, S. V. Buldyrev, S.-H. Chen, P. H. Poole, F. Sciortino, and H. E. Stanley, Proc. Natl. Acad. Sci. U.S.A. **102**, 16558 (2005).
[20] C. A. Angell, Science **319**, 582 (2008).
[21] S.-H. Chen, J. Liu, Y. Zhang, E. Fratini, P. Baglioni, A. Faraone, and E. Mamontov, J. Chem. Phys. **125**, 171103 (2006).
[22] M. Lagi, X. Chu, C. Kim, F. Mallamace, P. Baglioni, and S.-H. Chen, J. Phys. Chem. B **112**, 1571 (2008).
[23] D. N. LeBard and D. V. Matyushov, J. Phys. Chem. B **112**, 5218 (2008).
[24] D. N. LeBard and D. V. Matyushov, J. Chem. Phys. **128**, 155106 (2008).
[25] Y. Xue, M. Okvist, O. Hansson, and S. Young, Protein Sci. **7**, 2099 (1998).
[26] W. L. Jorgensen, J. Chandrasekhar, J. D. Madura, R. W. Impey, and M. L. Klein, J. Chem. Phys. **79**, 926 (1983).
[27] H. J. C. Berendsen, J. P. M. Postma, W. F. van Gunsteren, A. DiNola, and J. R. Haak, J. Chem. Phys. **81**, 3684 (1984).
[28] M. Krishnan, V. Kurkal-Siebert, and J. Smith, J. Phys. Chem. B **112**, 5522 (2008).
[29] D. Vitkup, D. Ringe, G. A. Petsko, and M. Karplus, Nat. Struct. Biol. **7**, 34 (2000).
[30] M. Tarek and D. J. Tobias, Phys. Rev. Lett. **88**, 138101 (2002).
[31] P. K. Ghorai and D. V. Matyushov, J. Chem. Phys. **124**, 144510 (2006).
[32] J. L. Green, J. Fan, and C. A. Angell, J. Phys. Chem. **98**, 13780 (1994).
[33] P. W. Fenimore, H. Frauenfelder, B. H. McMahon, and R. D. Young, Proc. Natl. Acad. Sci. U.S.A. **101**, 14408 (2004).
[34] L. Nilsson and B. Halle, Proc. Natl. Acad. Sci. U.S.A. **102**, 13867 (2005).
[35] K. Binder and D. W. Heermann, *Monte Carlo Simulation in Statistical Mechanics* (Springer-Verlag, Berlin, 1992).
[36] D. V. Matyushov, Mol. Phys. **79**, 795 (1993).
[37] D. Chandler, Nature (London) **437**, 640 (2005).
[38] D. M. Huang and D. Chandler, Proc. Natl. Acad. Sci. U.S.A. **97**, 8324 (2000).
[39] N. V. Prabhu and K. A. Sharp, Annu. Rev. Phys. Chem. **56**, 521 (2005).
[40] D. V. Matyushov, Chem. Phys. **351**, 46 (2008).
[41] B. K. P. Scaife, *Principles of Dilectrics* (Clarendon, Oxford, 1998).
[42] J. Mijović, Y. Bian, R. A. Gross, and B. Chen, Macromolecules **38**, 10812 (2005).
[43] F. Bruni and S. F. Pagnotta, Phys. Chem. Chem. Phys. **6**, 1912 (2004).
[44] A. Levstik, C. Filipič, Z. Kutnjak, G. Careri, G. Consolini, and F. Bruni, Phys. Rev. E **60**, 7604 (1999).
[45] P. M. Suherman and G. Smith, J. Phys. D **36**, 336 (2003).
[46] C. Y. Lee, J. A. McCammon, and P. J. Rossky, J. Chem. Phys. **80**, 4448 (1984).
[47] M. Gerstein and R. M. Lynden-Bell, J. Phys. Chem. **97**, 2982 (1993).
[48] J. Swenson, H. Jansson, J. Hedsröm, and R. Bergman, J. Phys.: Condens. Matter **19**, 205109 (2007).
[49] G. Caliskan, R. M. Briber, D. Thirumalai, V. Garcia-Sakai, S. A. Woodson, and A. P. Sokolov, J. Am. Chem. Soc. **128**, 32 (2005).
[50] A. L. Tournier, J. Xu, and J. C. Smith, Biophys. J. **85**, 1871 (2003).
[51] S. K. Sinha, S. Chakraborty, and S. Bandyopadhyay, J. Phys. Chem. B **112**, 8203 (2008).
[52] K. L. Ngai and S. Capaccioli, J. Phys.: Condens. Matter **19**, 205114 (2007).
[53] I. Brovchenko, A. Geiger, and A. Oleinikova, J. Chem. Phys. **123**, 044515 (2005).
[54] A. L. Tournier and J. C. Smith, Phys. Rev. Lett. **91**, 208106 (2003).
[55] L. Meinhold and J. C. Smith, Phys. Rev. E **72**, 061908 (2005).
[56] A. Oleinikova, N. Smolin, and I. Brovchenko, J. Phys. Chem. B **110**, 19619 (2006).
[57] Y. He and A. G. Markelz, e-print arXiv:0807.3528v1.
[58] V. M. Dadarlat and C. B. Post, Biophys. J. **91**, 4544 (2006).